

Optimization of the optical properties of circular lattice As₂Se₃ photonic crystal fibers over a wide range of wavelengths

Duc Hoang Trong¹, Bao Tran Le Tran², Long Vu Dinh², Lanh Chu Van², Thuy Nguyen Thi^{1,*}



Use your smartphone to scan this QR code and download this article

ABSTRACT

In this paper, the dispersion and nonlinear properties of circular lattice photonic crystal fibers with As₂Se₃ substrates are investigated over a wide wavelength range up to 11 μm. By solving Maxwell's wave equations using the full-vector finite-difference eigenmode method, the optical properties of the PCFs have been analyzed in detail and compared with recent studies. All-normal and anomalous dispersions with small values, very high nonlinear coefficients, and very low confinement losses have been achieved in comparison with the previous publications. The characteristic quantities of the proposed optimal fibers were obtained at the pump wavelength of 2.35 μm including flat dispersion and as small as 1.069 ps/nm.km, non-linear coefficients as high as 62023.377 W⁻¹.km⁻¹, and confinement losses as low as 10⁻²¹ dB/m, making them suitable for use in a broadband super-continuum generation process with a low input power. These fibers are suitable low-cost all-fiber laser sources that effectively replace the current glass fibers.

Key words: PCFs with As₂Se₃ substrates, small dispersion, very high nonlinear coefficient, low confinement loss, supercontinuum generation

INTRODUCTION

In supercontinuum (SC) generation, photonic crystal fibers (PCFs) are an excellent nonlinear medium for the nonlinear interactions that occur when the fiber is excited by an ultrashort pulse of laser light. These input optical pulses undergo extreme nonlinear spectral expansion to yield a spectrally continuous white light output while passing through the PCFs¹. This is the result of nonlinear interactions such as self-phase modulation (SPM), optical wave breaking (OWB), cross-phase modulation (CPM), self-steepening, four-wave mixing (FWM), stimulated Raman scattering (SRS), and dispersion effects. These effects are strongly dominated by the dispersions and nonlinear properties of the PCFs.

In recent years, a large number of²⁻¹¹ publications on SC via silica-based PCFs have demonstrated the ability of said PCFs to generate broad, flat, smooth, and highly coherent SC spectra, which opens up a wide range of applications such as telecommunications, optical metrology, optical coherence tomography, biomedical imaging, biomedical sensor, nonlinear microscopy, cosmological studies, ultra-short pulses, and frequency combs generation¹²⁻¹⁹. However, due to silica's high matter absorption, the SC spectrum has failed to extend beyond 2.5 μm and has not extended to the mid-infrared (MIR) wavelength range (2–20 μm). To enhance the SC spectrum

scalability, chalcogenide glasses have been proven to be the most promising²⁰ because they have high optical transparency up to 25 μm in the MIR region²¹ and extensive linear and nonlinear refractive indices²². Among the chalcogenide glasses compositions, As₂Se₃ exhibits optical transparency in the range of 0.85–17.5 μm, and its attenuation coefficient is low (less than 1 cm⁻¹)²¹. As₂Se₃ glass has a high nonlinear refractive index, twice that of silica²³. Therefore, many research groups have chosen As₂Se₃ as an excellent substrate to design and fabricate PCFs and investigate the SC process. The work²⁴ obtained an all-normal, nearly zero flat-top dispersion with a triangular-core photonic crystal fiber in As₂Se₃-based chalcogenide glass. This optimum fiber gives a nonlinear coefficient as high as 5449 W⁻¹.km⁻¹ with an effective mode area of 6.15 μm² at 4.5 μm pump wavelength and offers 0.3 dB/cm loss for the propagating mode. By optimizing the structure parameters, the article²⁵ also demonstrated the ability to achieve high nonlinear coefficients for the PCFs up to 2079 W⁻¹.km⁻¹ at a wavelength of 2 μm. The confinement losses are still lower than 0.025 × 10⁻² dB/cm. With a traditional hexagonal structure, the publication²⁶ showed that the nonlinear coefficient for this PCF is 1610 W⁻¹.km⁻¹ with an effective mode area of 6.59 μm² where the dispersion value is 19.92 ps/nm.km at the pump wavelength. When

¹University of Education, Hue University, 34 Le Loi, Hue City, Viet Nam

²Department of Physics, Vinh University, 182 Le Duan, Vinh City, Viet Nam

Correspondence

Thuy Nguyen Thi, University of Education, Hue University, 34 Le Loi, Hue City, Viet Nam

Email: ntthuy@hueuni.edu.vn

History

- Received: 2022-08-19
- Accepted: 2022-11-30
- Published: 2023-01-20

DOI : 10.32508/stdj.v25i4.3989



Copyright

© VNUHCM Press. This is an open-access article distributed under the terms of the Creative Commons Attribution 4.0 International license.



Cite this article : Trong D H, Tran B T L, Dinh L V, Van L C, Thi T N. Optimization of the optical properties of circular lattice As₂Se₃ photonic crystal fibers over a wide range of wavelengths. *Sci. Tech. Dev. J.*; 2022, 25(4):2581-2593.

studying the process of SC generating a broad spectrum, the work by²⁷ demonstrated that the “average loss in the wavelength range of 2.5–12.0 μm is about 4×10⁻² dB/cm” for the PCF consisting of an As₂Se₃ core and As₂Se₃S cladding determined experimentally. The diversity in dispersion properties of As₂Se₃ PCF with a small hollow core are also demonstrated by the work of²⁸ with the anomalous dispersion of one zero dispersion wavelength (ZDW) and two ZDWs. The dispersions are quite flat in the wavelength range investigated, 1–10 μm. The confinement losses of the PCFs are smaller than 10⁻² dB/cm for the wavelengths up to ~5 μm. With the proposed two optimal fibers, the paper²⁹ has shown the dispersion and nonlinear properties that are beneficial for the SC generation of As₂Se₃ solid core PCFs. With an all-normal dispersion, the value changes “from -60 to -1.7 ps/nm.km in the wavelength range of 3–4.6 μm, and it is further flat in the longer wavelength range. The maximum value of anomalous dispersion is 11.2 ps/nm.km at 5.7 μm”. A rather large nonlinear coefficient is also found in these PCFs with values ranging from 695 to 2850 W⁻¹.km⁻¹ and effective mode areas varying from 11.5 to 50 μm² respectively in the wide wavelength region of 2–11 μm. A confinement loss of a few dB/cm is also observed for these optimal fibers.

In this work, we simulate As₂Se₃ solid-core PCFs with a circular lattice and numerically investigate its optical properties in the wide wavelength region from 2 to 11 μm. Diversity in dispersion with all-normal and anomalous dispersions was obtained by varying the lattice parameters. At the same time, the PCFs exhibit rather high nonlinearity with a nonlinear coefficient of up to 62023.377 W⁻¹.km⁻¹ at the pump wavelength. In particular, it is easy to control the confinement loss with the variation of the filling factor d/Λ resulting in a very small value of about 10⁻²¹ dB/m. These characteristic properties are well-suited for generating broad-spectrum SCs in the mid-infrared (MIR) wavelength.

MATERIALS-METHODS

The As₂Se₃ solid-core PCFs are designed by Lumerical Mode Solutions (LMS) software using the finite difference eigenmode method. The cross-section of the optical fiber is divided into small rectangular parts to reduce the meshing error of the simulations. The Maxwell wave equation is used to calculate the modes of light propagating in an optical fiber with the boundary condition that the layers are perfectly matched.

This can reduce the loss, thereby increasing the accuracy of the structural simulation and optical properties of the fibers. To simulate these PCFs, first the coefficients of the refractive index of As₂Se₃ as a function of wavelength according to the Sellmeier equation³⁰ (Equation (1)) are entered into the LMS material database. Next, the circular lattice was selected from the available data to design the initial geometry for the PCFs, and the air was set up for parallel holes along with the fiber. Finally, we carefully re-examine the structural parameters and simulate the propagation of light along with the fiber.

$$n^2 - 1 = \frac{2.234921\lambda^2}{\lambda^2 - 0.24164^2} + \frac{0.347441\lambda^2}{\lambda^2 - 19^2} + \frac{1.308575\lambda^2}{\lambda^2 - 4 \times 0.24164^2} \quad (1)$$

The circular lattice cross-section of the fiber is depicted as shown in **Figure 1a**. Eight layers of parallel air holes along the fiber length in the cladding are cyclically arranged around a solid core of diameter D_c . The small core is determined by the formula $D_c = 2\Lambda - d$, which helps the electromagnetic field be better confined in the core. The distance between two adjacent air holes in the lattice constant Λ and the diameter of each air hole is defined as d . We use the filling factor d/Λ to investigate the variation of dispersion and nonlinear properties with wavelength. The selected parameters are $\Lambda = 1.0; 1.5; 2.0; 2.5 \mu\text{m}$, while d/Λ varies from 0.3 to 0.8 with each step 0.5. **Figure 1b** shows the well-confined light modes in the cores of PCFs with $\Lambda = 2.5 \mu\text{m}$ and $d/\Lambda = 0.65$. The relationship between the real parts of the refractive index of As₂Se₃ and the wavelength is shown in **Figure 1c**.

RESULTS

In SC generation using PCF, the optical properties including the effective refractive index, dispersion, effective mode area, nonlinear coefficient, and confinement loss play an important role in the SC spectrum expansion. Each feature will govern the spectral expansion in its own way, so it will be difficult to optimize all properties of PCF simultaneously. The larger the effective refractive index difference between the core and the cladding, the better the light is confined in the core, resulting in a lower loss. The real part of the effective refractive index ($\text{Re}[n_{eff}]$) of PCFs is a function of wavelength as depicted in **Figure 2**. The increase in wavelength causes the $\text{Re}[n_{eff}]$ to decrease due to the stronger penetration of low-frequency modes into the cladding of the PCFs. For each case where the lattice constant is

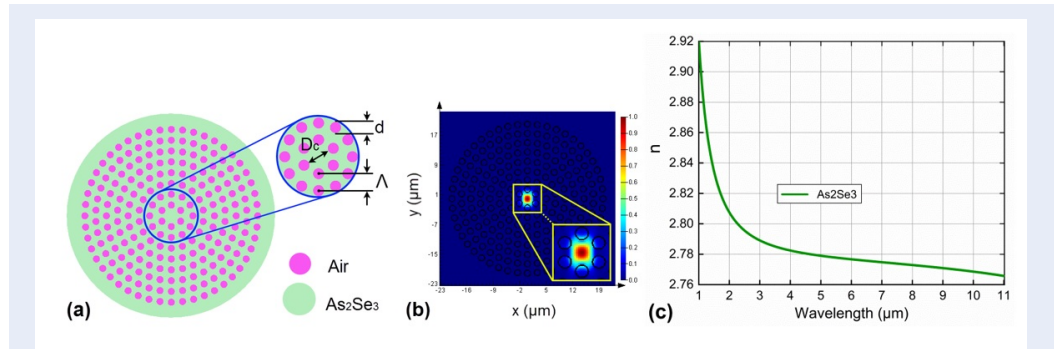


Figure 1: The cross-section geometrical structure of the PCF; the air holes are arranged in a circle and parallel to the core (a), the light is confined in the core of PCF with $\Lambda = 2.5 \mu\text{m}$ and $d/\Lambda = 0.65$ (b), and the real parts of the refractive index n of As_2Se_3 depend on the wavelength (c).

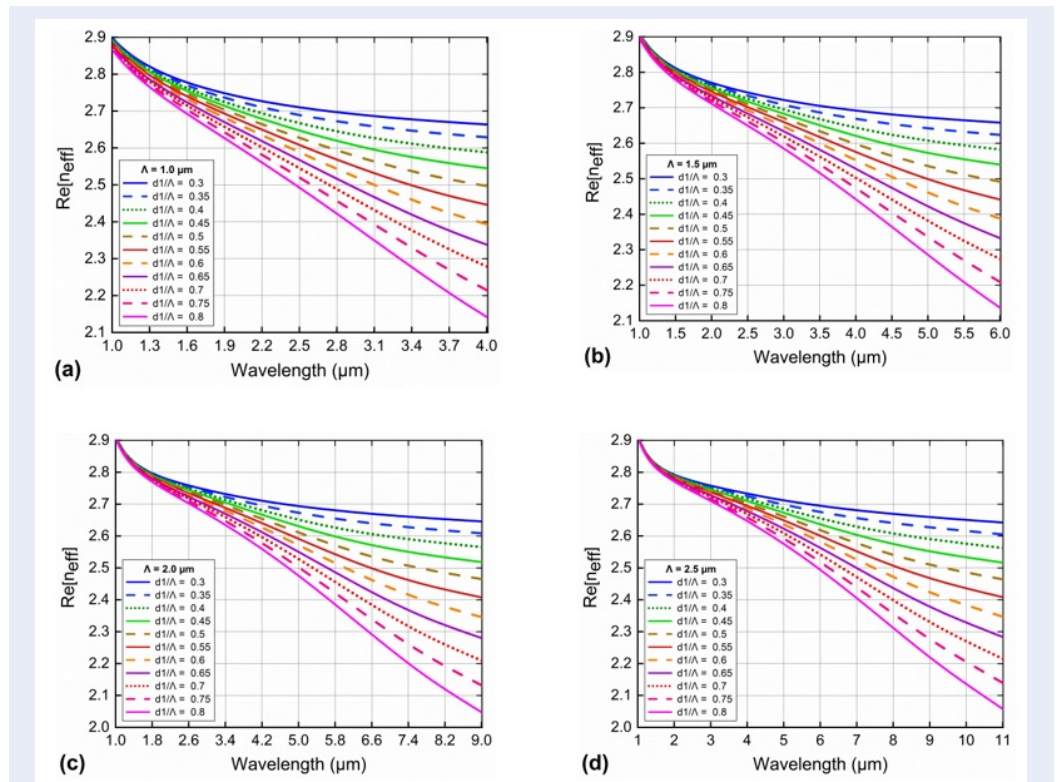


Figure 2: The real part of the effective refractive index decreases with the increasing wavelength which is a function of d/Λ for various Λ , $\Lambda = 1.0 \mu\text{m}$ (a), $1.5 \mu\text{m}$ (b), $2.0 \mu\text{m}$ (c), and $2.5 \mu\text{m}$ (d).

fixed, $\text{Re}[n_{eff}]$ decreases as the filling factor d/Λ increases. Meanwhile, $\text{Re}[n_{eff}]$ increases as the lattice constant increases if d/Λ is fixed. The refractive index of the medium's material changes when a high-energy input pulse passes through the nonlinear medium. The interaction of the input pulse with the nonlinear medium is stronger if the fiber has a smaller core, resulting in a small $\text{Re}[n_{eff}]$ ³¹.

The value of $\text{Re}[n_{eff}]$ at a pump wavelength of 3.0 μm is shown in **Table 1**. The maximum and minimum values of $\text{Re}[n_{eff}]$ are 2.758 and 2.374 respectively where structure $\Lambda = 2.5 \mu\text{m}$, $d/\Lambda = 0.3$, and $\Lambda = 1.0 \mu\text{m}$, $d/\Lambda = 0.8$.

The chromatic dispersion of an optical material is the phenomenon where the phase velocity and group velocity of light propagating in a nonlinear medium depend on the optical frequency due to the interaction of the light with the electrons of the medium. Flat dispersion in a wide wavelength range, with small dispersion values, and a reasonable ZDWs shift are among the desirable characteristics for efficient SC generation. The chromatic dispersion is calculated through the second derivative of the effective refractive index for wavelength, which is determined as follows³²:

$$D_c = -\frac{\lambda}{c} \frac{d^2 \text{Re}[n_{eff}]}{d\lambda^2} \quad (2)$$

where $\text{Re}[n_{eff}]$ is the real part of n_{eff} which is the effective index of a guided mode calculated by the means of the Finite Difference Eigenmode (FDE) method, and where c is the velocity of light in a vacuum.

Figure 3 displays the dependence of the dispersion on the wavelength of the PCFs with the change in the lattice constant Λ and filling factor d/Λ . It can be seen that the PCFs have large lattice constants and that the compatible wavelength region is up to 11 μm . This is a very favorable condition for the application of PCFs in the MIR wavelength range. Diversity in the dispersion properties is easily found in these PCFs, which manifest in all-normal and anomalous dispersion regimes with both one and two ZDWs.

For $\Lambda = 1.0 \mu\text{m}$, we obtained seven all-normal dispersion curves with $d/\Lambda \leq 0.6$ and four anomalous dispersion curves with two ZDWs where the d/Λ is greater than 0.6. The anomalous dispersion curve with $d/\Lambda = 0.65$ is the flattest and has a rather small value of 1.069 ps/nm.km at the pump wavelength of 2.35 μm . This value is much smaller than the work^{24,26,29}. In work²⁹, #F₁ has an all-normal dispersion with a value varying from -60 to -1.7 ps/nm.km in the wavelength range of 3 - 4.6 μm , which is 56 to 1.5 times the dispersion value of fiber $\Lambda = 1.0 \mu\text{m}$,

$d/\Lambda = 0.65$. In the wavelength region of 2.35 - 4.0 μm , the values of the all-normal dispersion curve are 5 to 19 times smaller than in publication²⁴ and 4 to 8 times smaller than in work²⁶. The number of all-normal and anomalous dispersion curves changes as Λ and d/Λ change. In particular, the number of all-normal dispersion curves decreases as Λ increases which means that the number of anomalous dispersion curves increases. Furthermore, the ZDWs shift towards the long wavelength, making the pump wavelength selection easier. For $\Lambda = 2.5 \mu\text{m}$, only two all-normal dispersion curves are found. In this case, the survey wavelength extended to 11 μm is very convenient for the application of SC in the MIR region. At the same time, the ZDWs of the PCFs in this case, which is in the range of 4.939-8.005 μm , are very suitable when choosing the pumping wavelength in the MIR region. The shifting of the ZDWs to the long wavelength region is shown in **Table 2**.

The nonlinear effects that occur when the high-intensity narrow pulse interacts with a nonlinear medium such as PCF depends strongly on the dispersion properties of the PCFs, governing the SC spectral expansion. Typically, PCFs have an all-normal dispersion and the SC spectrum is extended by the effect of SPM followed by OWB. For PCFs with an anomalous dispersion, the soliton effect plays a major role in spectral broadening. Therefore, the dispersion diversity of our PCF designs will guide the way that the SC spectrum is generated.

For a nonlinear optical medium, the higher the nonlinear coefficient, the more beneficial it is to expand the SC spectrum. Furthermore, the nonlinearity of the medium also directly affects the input pulse peak power. The nonlinearity of the environment is evaluated through the nonlinear coefficient (γ). For PCFs, it is expressed as a function of wavelength and can be estimated by the formula¹:

$$\gamma(\lambda) = 2\pi \frac{n_2}{\lambda A_{eff}} \quad (3)$$

where n_2 is the nonlinear refractive index of As_2Se_3 , $n_2 = 2.24 \times 10^{-17} \text{ m}^2 \cdot \text{W}^{-1}$ ³³, and A_{eff} is the effective mode area for the fundamental mode of the fiber. It is also a nonlinear characteristic of PCFs. The effective mode area is the quantitative measure of the area that a waveguide or fiber mode effectively covers in the transverse dimensions, and it is determined through the transverse electric field over the cross-section of the PCF¹:

$$A_{eff} = \frac{(\int_{-\infty}^{\infty} \int_{-\infty}^{\infty} |E|^2 dx dy)^2}{\int_{-\infty}^{\infty} \int_{-\infty}^{\infty} |E|^4 dx dy} \quad (4)$$

Table 1: The real part of the effective refractive index at 3.0 μm wavelength of PCFs with various the d/Λ and Λ

d/Λ	Re[n _{eff}]			
	$\Lambda = 1.0 \mu\text{m}$	$\Lambda = 1.5 \mu\text{m}$	$\Lambda = 2.0 \mu\text{m}$	$\Lambda = 2.5 \mu\text{m}$
0.3	2.69	2.722	2.744	2.758
0.35	2.663	2.709	2.737	2.754
0.4	2.633	2.695	2.731	2.750
0.45	2.603	2.683	2.724	2.746
0.5	2.573	2.671	2.718	2.742
0.55	2.544	2.66	2.711	2.737
0.6	2.514	2.647	2.704	2.733
0.65	2.483	2.634	2.697	2.728
0.7	2.451	2.620	2.689	2.723
0.75	2.414	2.603	2.679	2.716
0.8	2.374	2.586	2.669	2.710

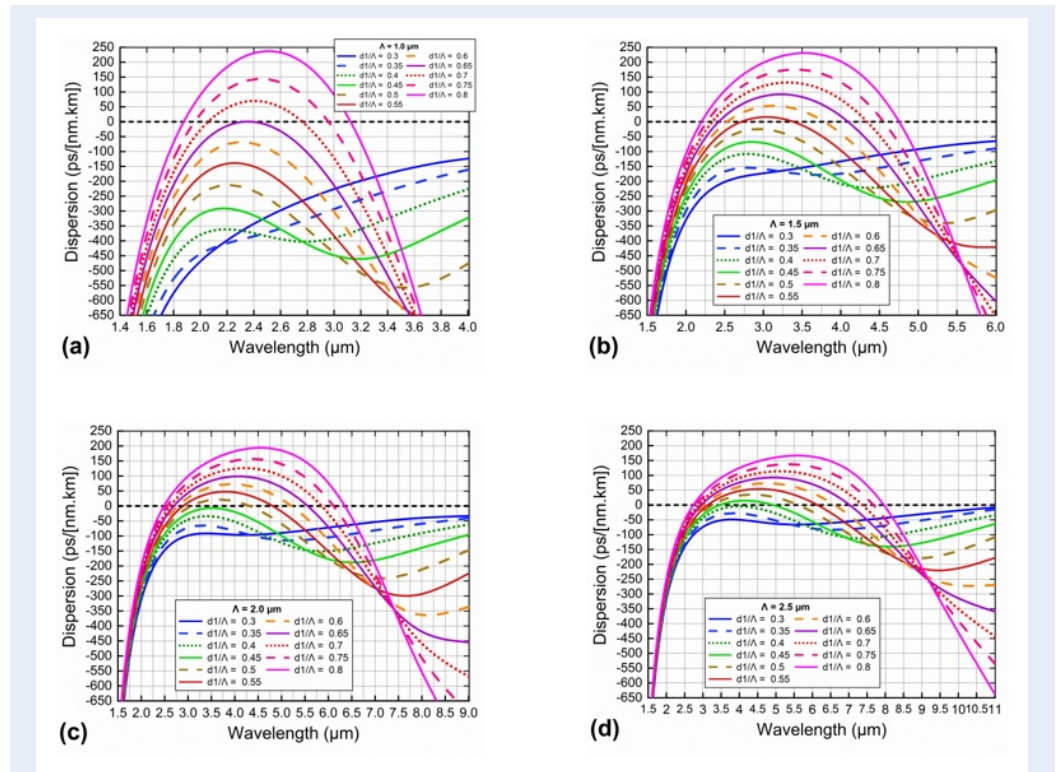


Figure 3: The chromatic dispersion of the PCFs varies with the wavelength for different values of d/Λ and Λ , with $\Lambda = 1.0 \mu\text{m}$ (a), $1.5 \mu\text{m}$ (b), $2.0 \mu\text{m}$ (c), and $2.5 \mu\text{m}$ (d).

Table 2: The ZDWs of PCFs with various d/Λ and Λ

d/Λ	$\Lambda = 1.0 \mu\text{m}$		$\Lambda = 1.5 \mu\text{m}$		$\Lambda = 2.0 \mu\text{m}$		$\Lambda = 2.5 \mu\text{m}$	
	ZDW _{s1}	ZDW _{s2}						
0.3								
0.35								
0.4								
0.45							3.459	4.939
0.5					3.060	4.333	3.252	5.622
0.55			2.713	3.395	2.892	4.815	3.130	6.151
0.6			2.528	3.796	2.781	5.220	3.032	6.642
0.65	2.317	2.408	2.422	4.096	2.697	5.566	2.952	7.038
0.7	2.058	2.765	2.338	4.344	2.618	5.880	2.875	7.411
0.75	1.957	2.961	2.268	4.559	2.552	6.121	2.805	7.689
0.8	1.875	3.124	2.200	4.769	2.485	6.399	2.735	8.005

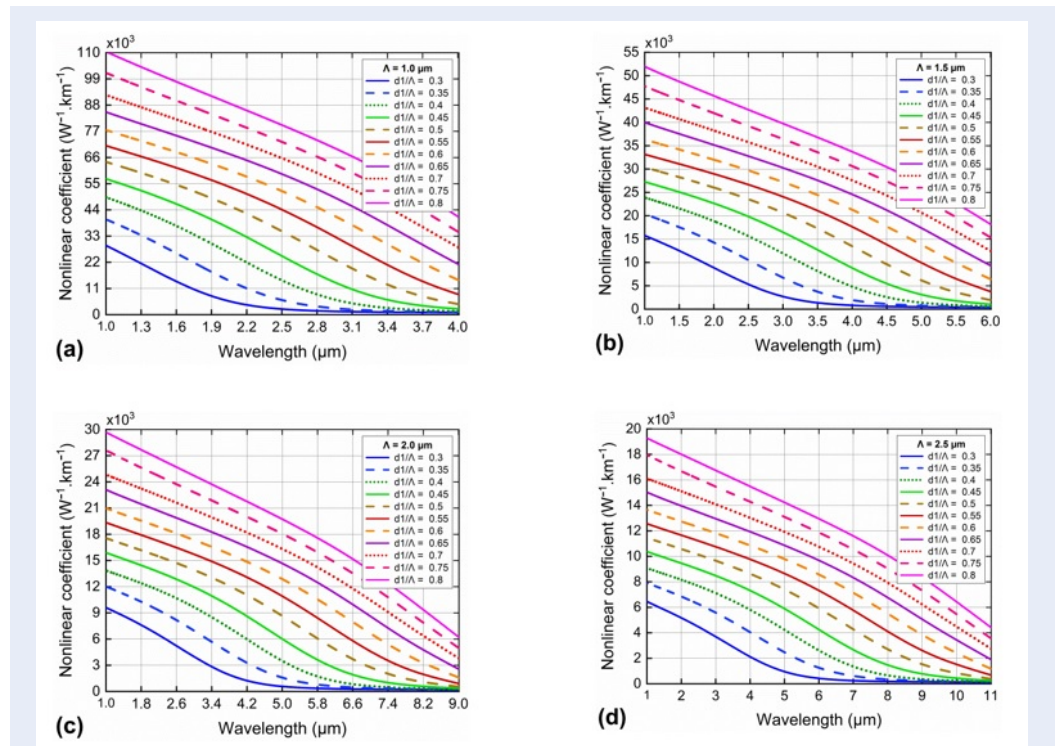


Figure 4: The nonlinear coefficient of PCFs with various d/Λ for the $\Lambda = 1.0 \mu\text{m}$ (a), $1.5 \mu\text{m}$ (b), $2.0 \mu\text{m}$ (c), and $2.5 \mu\text{m}$ (d).

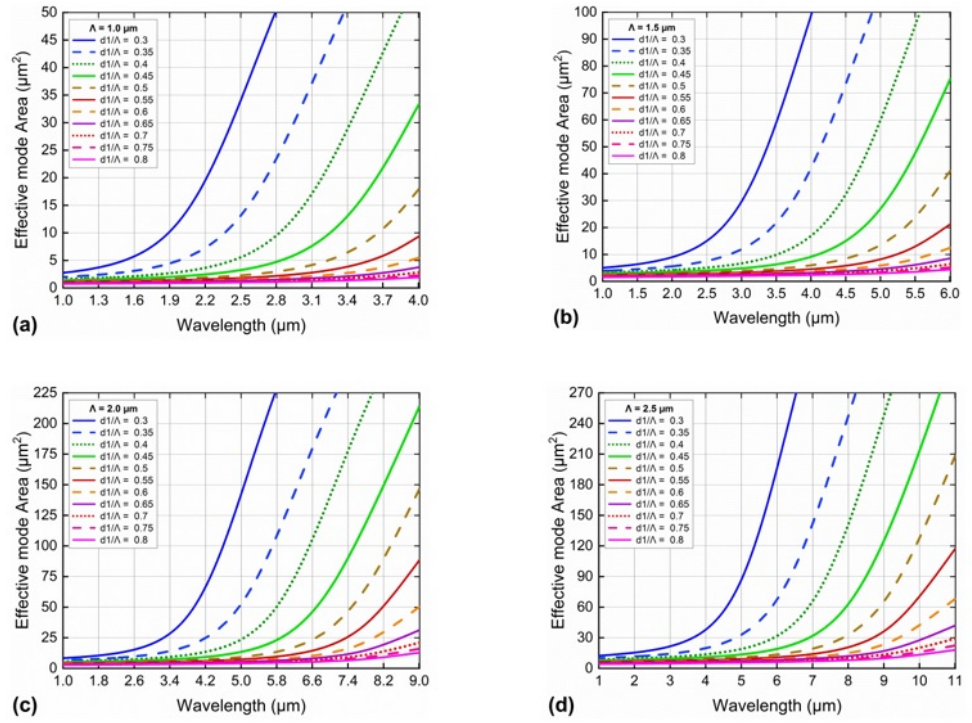


Figure 5: The effective mode area of PCFs varies with wavelength for different values of d/Λ and Λ , with $\Lambda = 1.0 \mu\text{m}$ (a), $1.5 \mu\text{m}$ (b), $2.0 \mu\text{m}$ (c), and $2.5 \mu\text{m}$ (d).

The relationship between the nonlinear coefficient, effective mode area, and wavelength are described in the graphs in **Figure 4** and **Figure 5**.

Thanks to highly nonlinear substrates such as As_2Se_3 , the PCFs exhibit high nonlinearity. Nonlinear coefficients up to hundreds of thousands of $\text{W}^{-1}.\text{km}^{-1}$ are achieved in the short wavelength region for structures with small Λ ($\Lambda = 1.0 \mu\text{m}$). In all cases, the nonlinear coefficient decreases in the long wavelength region which equates to an increase in the effective mode area since the two quantities are inversely proportional. The cause of the reduction of the nonlinear coefficient at long wavelengths is due to the low-frequency light modes easily leaking out of the PCF cladding. Therefore, the choice of pump wavelength in the SC study is necessary to obtain a suitably high nonlinear coefficient at a given wavelength value. When Λ is constant, the nonlinear coefficient increases with the increase in d/Λ . The light confinement of small core PCFs is better than that of large cores, resulting in higher nonlinear coefficients.

The values of the nonlinearity coefficient and effective mode area at a $3.0 \mu\text{m}$ wavelength are calculated and presented in Tables 3 and 4. It can be seen that the

nonlinear coefficient varies in the range of 3698.75 to $68812.53 \text{ W}^{-1}.\text{km}^{-1}$. These values are much higher than the values in some of the previous publications on As_2Se_3 -based PCF²⁴⁻²⁹. Nonlinear coefficients of a few hundred $\text{W}^{-1}.\text{km}^{-1}$ to several thousand of $\text{W}^{-1}.\text{km}^{-1}$ were found in these publications. Similarly, the maximum and minimum effective mode areas are 60.381 and $1.162 \mu\text{m}^2$ for structures with $\Lambda = 1.0 \mu\text{m}$, $d/\Lambda = 0.3$, and $\Lambda = 1.0 \mu\text{m}$, $d/\Lambda = 0.8$ respectively.

The very high and very small values of the nonlinear coefficient and effective mode area are essential factors in the selection of optimal PCF structures, which is beneficial when studying SC generation.

Confinement loss (L_c) is the loss arising from the leaky nature of the modes and the non-perfect structure of the PCF fiber. For PCFs, the factors such as wavelength, the number of hole rings, hole size, lattice type, and lattice constant govern the value of the confinement loss. This can be determined from the imaginary part of the effective refractive index of the PCF by³⁴

$$L_c = 8.686 \frac{2\pi}{\lambda} \text{Im} [n_{eff}(\lambda)] \quad (5)$$

Table 3: The values of nonlinear coefficients at 3.0 μm wavelength of PCFs with various d/Λ and Λ

d/Λ	γ (W ⁻¹ .km ⁻¹)			
	Λ = 1.0 μm	Λ = 1.5 μm	Λ = 2.0 μm	Λ = 2.5 μm
0.3	1326.064	2715.213	3981.890	3698.750
0.35	2487.432	6741.244	6959.631	5584.340
0.4	5759.833	11954.672	9646.789	7119.574
0.45	12564.570	16497.341	11949.285	8484.345
0.5	21909.123	20664.465	13913.406	9663.513
0.55	31451.521	24085.371	15707.346	10754.182
0.6	40197.176	27235.001	17351.661	11824.578
0.65	48016.513	30274.301	19081.377	12956.791
0.7	55074.238	33207.383	20781.652	14083.392
0.75	61918.597	36446.197	22809.314	15475.677
0.8	68812.530	39754.817	24713.967	16749.932

Table 4: The values of effective mode area at 3.0 μm wavelength of PCFs with various d/Λ and Λ

d/Λ	A _{eff} (μm ²)			
	Λ = 1.0 μm	Λ = 1.5 μm	Λ = 2.0 μm	Λ = 2.5 μm
0.3	60.381	29.587	20.113	21.623
0.35	32.348	11.890	11.492	14.315
0.4	14.048	6.693	8.287	11.227
0.45	6.416	4.847	6.689	9.420
0.5	3.664	3.869	5.745	8.271
0.55	2.547	3.319	5.088	7.432
0.6	1.991	2.935	4.606	6.759
0.65	1.666	2.640	4.189	6.168
0.7	1.452	2.407	3.846	5.675
0.75	1.291	2.193	3.504	5.164
0.8	1.162	2.010	3.234	4.772

Figure 6 denotes the confinement loss characteristics of the fundamental mode for PCFs. L_c increases with increasing wavelength. The modes leaking out of the core into the cladding or between the air holes causes the value of confinement loss to increase in the long wavelength region. In the case of a fixed Λ , the change in d/Λ also changes the value of L_c . As d/Λ increases, L_c decreases. However, in all cases, the value of confinement loss is very small when d/Λ is greater than 0.55. Table 5 indicates the value of L_c at 3.0 μm. The structures $\Lambda = 1.0 \mu\text{m}$, $d/\Lambda = 0.3$ and $\Lambda = 2.0 \mu\text{m}$, $d/\Lambda = 0.8$ give the maximum and minimum confinement loss values of 3.97×10^3 and 6.3×10^{-21} dB/m

at 3.0 μm wavelength. Some of the previous publications^{24,28,29} have shown confinement as small as a few dB/m, even a few tens of dB/m in the wavelength region from 2.0 to 5.0 μm, which is one of the favorable conditions in which to generate a broad SC spectrum. For PCFs with lattice constants greater than ($\Lambda = 1.5, 2.0, 2.5 \mu\text{m}$), the values of the confinement losses are 10^{-3} to 10^{-21} dB/m. These values are very small, specifically much smaller than some of the previous publications on As₂Se₃-based PCF²⁴⁻²⁹.

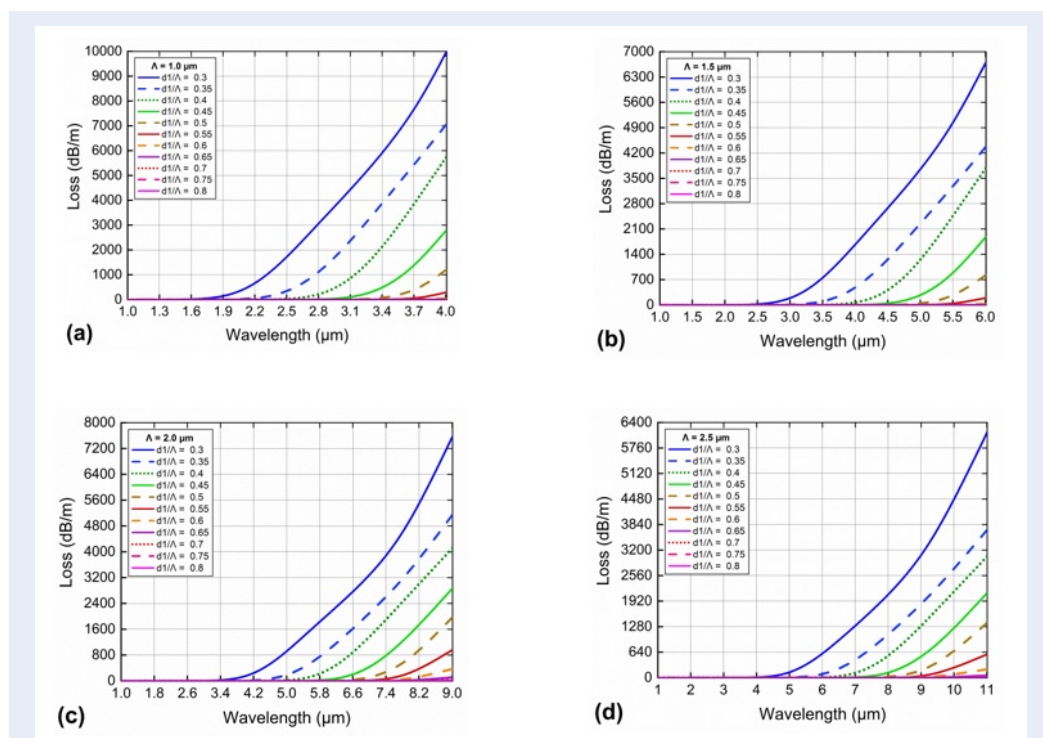


Figure 6: The confinement loss of PCFs varies according to wavelength for the different values of d/Λ and Λ with $\Lambda = 1.0 \mu\text{m}$ (a), $1.5 \mu\text{m}$ (b), $2.0 \mu\text{m}$ (c), and $2.5 \mu\text{m}$ (d).

Table 5: The values of confinement loss at $3.0 \mu\text{m}$ wavelength of PCFs with various d/Λ and Λ

d/Λ	L_c (dB/m)			
	$\Lambda = 1.0 \mu\text{m}$	$\Lambda = 1.5 \mu\text{m}$	$\Lambda = 2.0 \mu\text{m}$	$\Lambda = 2.5 \mu\text{m}$
0.3	3.97×10^3	1.88×10^2	4.000×10^0	2.102×10^{-1}
0.35	1.91×10^3	8.98×10^0	5.019×10^{-2}	1.397×10^{-3}
0.4	5.70×10^2	1.65×10^{-1}	4.337×10^{-4}	9.309×10^{-6}
0.45	5.28×10^1	1.86×10^{-3}	2.557×10^{-6}	4.736×10^{-8}
0.5	2.84×10^0	1.42×10^{-5}	1.157×10^{-8}	1.748×10^{-10}
0.55	8.07×10^{-2}	7.97×10^{-8}	3.821×10^{-11}	3.743×10^{-13}
0.6	1.69×10^{-3}	3.72×10^{-10}	9.998×10^{-14}	6.165×10^{-16}
0.65	3.29×10^{-5}	1.53×10^{-12}	1.737×10^{-3}	3.758×10^{-19}
0.7	5.44×10^{-7}	3.86×10^{-15}	-4.468×10^{-19}	5.943×10^{-19}
0.75	9.77×10^{-9}	6.72×10^{-18}	-7.630×10^{-19}	-6.542×10^{-19}
0.8	2.35×10^{-10}	-2.94×10^{-18}	-6.300×10^{-21}	-4.209×10^{-19}

DISCUSSION

Typically, PCFs possessing a flat all-normal dispersion will have advantages in terms of widening the SC spectrum which is smooth and highly coherent. However, the input peak power will be quite high. In contrast, PCF has an anomalous dispersion, enabling a broader SC spectrum. Although the input peak power is low, the spectrum is noisy. The occurrence of nonlinear effects when the ultra-short pulse propagates in a nonlinear medium strongly depends on the different dispersion regime of the PCF. Depending on the actual application, this means that we can choose the optimal structures with a flat dispersion that are suitable for SC generation. Furthermore, nonlinear properties such as the nonlinear coefficient, effective mode area, and confinement loss also contribute to the SC spectral generation efficiency by generating new wavelengths. The nonlinear coefficient is also the necessary key affecting the magnitude of the input peak power. Using small peak power to generate a broad SC spectrum is also the target of SC research groups. Based on the numerical analysis of the optical properties of As₂Se₃-based PCFs in the above sections, we chose three structures with a reasonable flat dispersion, small dispersion, and nonlinear properties suitable for use in SC generation application. We named the first structure $\Lambda = 1.0 \mu\text{m}$, $d/\Lambda = 0.65$ as #F₁, the second structure $\Lambda = 2.5 \mu\text{m}$, $d/\Lambda = 0.4$ as #F₂, and the third structure $\Lambda = 2.5 \mu\text{m}$, $d/\Lambda = 0.45$ as #F₃. The dispersion and nonlinear properties of the three optimal structures are presented in **Figure 7**.

(a) the all-normal and anomalous dispersion as a function of wavelength; the inset shows a partial dispersion curve with values of 1.069, -4.286, and 1.719 ps/nm.km at the corresponding pump wavelengths of 2.35, 4.0, and 3.5 μm .

(b) the nonlinear coefficient decreases with the increasing wavelength; the inset shows a partial nonlinear coefficient curve with values 62023.377, 5810.594, and 7932.324 $\text{W}^{-1}.\text{km}^{-1}$ at the corresponding pump wavelengths of 2.35, 4.0, and 3.5 μm .

(c) the effective mode area increases with the increasing wavelength; the inset shows a partial nonlinear coefficient curve with values 1.289, 13.766, and 10.077 μm^2 at the corresponding pump wavelengths of 2.35, 4.0, and 3.5 μm .

(d) the confinement loss increases with the increasing wavelength; the inset shows a partial nonlinear coefficient curve with values 6.767×10^{-10} , 1.21×10^{-3} , and 6.38×10^{-7} dB/m at the corresponding pump wavelengths of 2.35, 4.0, and 3.5 μm .

The values of the characteristic quantities of the three optimal structures are shown in **Table 6**. #F₁ fiber

has an anomalous dispersion with two ZDWs. The dispersion value is quite small at a 2.35 μm pump wavelength of 1.069 ps/nm.km. The #F₃ fiber also exhibits an anomalous dispersion mode but has one ZDW, where a rather small dispersion value of 1.719 ps/nm.km is found at the pump wavelength of 3.5 μm . These two fibers are expected to generate a wide SC spectrum with small peak power because of their high nonlinearity and very small confinement loss. The nonlinear coefficients of the two fibers at the pump wavelength are 62023.377 and 7932.324 $\text{W}^{-1}.\text{km}^{-1}$, respectively. The L_c value of the two fibers #F₁ and #F₃ is very small, about 10^{-10} and 10^{-7} dB/m. The #F₂ fiber has an all-normal dispersion mode which will enable SC with a broad spectrum that is smooth and with high coherence. The pump wavelength chosen is 4.0 μm which is quite ideal for SC generation in the MIR region. The dispersion magnitude is 4.286 ps/nm.km, which is larger than that of the two fibers #F₁ and #F₃. With the largest core diameter of the three fibers, #F₂ possesses the lowest nonlinear coefficient and the largest confinement loss.

With small dispersion values, a high nonlinear coefficient, and low confinement loss in comparison with the previous papers on SC generation based on As₂Se₃-based PCFs^{24-29,33}, the proposed optimal fibers are expected to produce a broad and highly coherent SC spectrum through typical nonlinear effects. It should be noted that it is difficult to simultaneously optimize the characteristic quantities of PCF, depending on the different application purposes used to select suitable PCFs.

CONCLUSIONS

We have designed forty-four As₂Se₃-based circular lattice PCFs, and their optical properties include the effective refractive index, dispersion, non-linear coefficient, effective mode area, and confinement loss, all of which were investigated numerically in detail. The all-normal and anomalous dispersions with one and two ZDWs were found to be flat and of a small value consistent with SC generation. Having a very high nonlinear coefficient and very small confinement loss compared to other publications are the outstanding advantages of this work. We have also proposed three optimal structures including $\Lambda = 1.0 \mu\text{m}$, $d/\Lambda = 0.65$, $\Lambda = 2.5 \mu\text{m}$, $d/\Lambda = 0.4$, and $\Lambda = 2.5 \mu\text{m}$, $d/\Lambda = 0.45$ with small dispersions, high nonlinear coefficients, and small confinement losses, all of which are very suitable for SC generation. These optimized structures can be used in low-cost all-fiber laser systems.

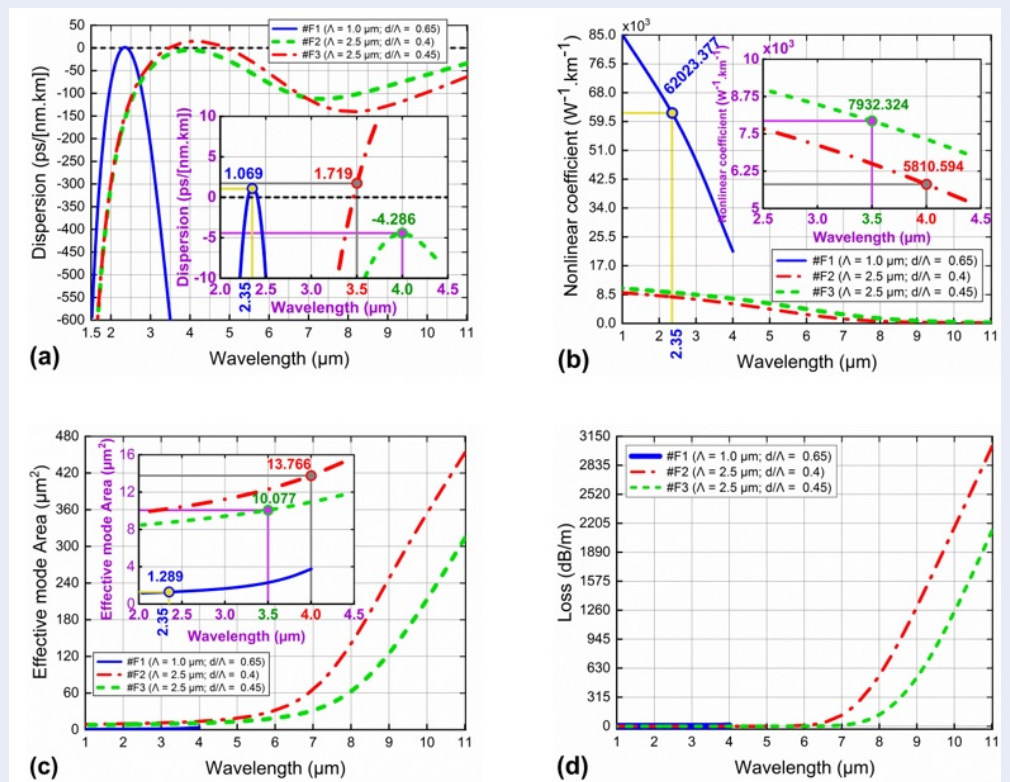


Figure 7: The optical properties of the three proposed optimal structures: #F₁ ($\Lambda = 1.0 \mu\text{m}$, $d_1/\Lambda = 0.65$), #F₂ ($\Lambda = 2.5 \mu\text{m}$, $d_1/\Lambda = 0.4$), and #F₃ ($\Lambda = 2.5 \mu\text{m}$, $d_1/\Lambda = 0.45$).

Table 6: The lattice parameters and the nonlinear characteristic values at the pump wavelength of three proposed PCFs

#	D_c	Λ	d_1/Λ	Pump wavelength	$\text{Re}[n_{eff}]$	A_{eff}	γ	D	L_c
	(μm)	(μm)		(μm)		(μm^2)	($\text{W}^{-1} \cdot \text{km}^{-1}$)	(ps/nm.km)	(dB/m)
#F1	1.35	1.0	0.65	2.35	2.593	1.289	62023.377	1.069	6.767×10^{-10}
#F2	4	2.5	0.4	4.0	2.717	13.766	5810.594	-4.286	1.21×10^{-3}
#F3	3.875	2.5	0.45	3.5	2.728	10.077	7932.324	1.719	6.38×10^{-7}

ABBREVIATIONS

SC: Supercontinuum
 PCFs: Photonic Crystal Fibers
 SPM: Self-Phase Modulation
 OWB: Optical Wave Breaking
 CPM: Cross-Phase Modulation
 FWM: Four-Wave Mixing
 SRS: stimulated Raman scattering
 MIR: Mid-Infrared
 ZDW: Zero Dispersion Wavelength
 LMS: Lumerical Mode Solutions
 FDE: Finite Difference Eigenmode

COMPETING INTERESTS

The authors declare that they have no conflicts of interest.

AUTHORS' CONTRIBUTIONS

Duc Hoang Trong: Writing manuscript, Plotting graph. Bao Tran Le Tran, Long Vu Dinh: Design and simulate the PCFs structures. Lanh Chu Van: Methodology, Data analysis, Supervision. Thuy Nguyen Thi: Data processing, Manuscript editing, Supervision.

ACKNOWLEDGEMENTS

This research is funded by Vietnam's Ministry of Education and Training (B2023-TDV-07).

REFERENCES

- Agrawal GP. Nonlinear Fiber Optics (5th edition). Academic Press, Elsevier. 2013; Available from: [10.1016/C2011-0-00045-5](https://doi.org/10.1016/C2011-0-00045-5).
- Lanh CV, Hieu VL, Nguyen DN, Ngoc VTM, Quang HD, Van TH, Thuy NT, Bien CV. Modelling of lead-bismuth gallate glass ultra-flattened normal dispersion photonic crystal fiber infiltrated with tetrachloroethylene for high coherence mid-infrared supercontinuum generation. *Laser Physics*. 2022;32(5):055102–12; Available from: <https://doi.org/10.1088/1555-6611/ac599b>.
- Lanh CV, Thuy NT, Duc HT, Bao TLT, Ngoc VTM, Trong DV, Trung LC, Quang HD, Khoa DQ. Comparison of supercontinuum spectrum generating by hollow core PCFs filled with nitrobenzene with different lattice types. *Optical and Quantum Electronics*. 2022;54(5):300; Available from: <https://doi.org/10.1007/s11082-022-03667-y>.
- Thuy NT, Duc HT, Bao TLT, Trong DV, Lanh CV. Optimization of optical properties of toluene-core photonic crystal fibers with circle lattice for supercontinuum generation. *Journal of Optics*. 2022; Available from: [10.1007/s12596-021-00802-y](https://doi.org/10.1007/s12596-021-00802-y).
- Khoa DX, Lanh CV, Van CL, Quang H D, Luu VM, Trippenbach M, Buczyński R. Influence of temperature on dispersion properties of photonic crystal fibers infiltrated with water. *Optical and Quantum Electronics*. 2017;49(2):87; Available from: <https://doi.org/10.1007/s11082-017-0929-3>.
- Lanh CV, Van TH, Van CL, Borzycki K, Khoa DX, Vu TQ, Trippenbach M, Buczyński R, Pniewski J. Supercontinuum generation in benzene-filled hollow-core fibers. *Optical Engineering*. 2021;60(11):116109; Available from: <https://doi.org/10.1117/1.OE.60.11.116109>.
- Quy HQ, Lanh CV. Spectrum Broadening of Supercontinuum Generation by fill Styrene in core of Photonic Crystal Fibers. *Indian Journal of Pure & Applied Physics*. 2021;59:522–527;.
- Bao Tran LT, Thuy NT, Ngoc VTM, Trung LC, Minh LV, Van CL, Khoa DX, Lanh CV. Analysis of dispersion characteristics of solid-core PCFs with different types of lattice in the claddings, infiltrated with ethanol. *Photonics Letters of Poland*. 2020;12(4):106–108; Available from: <https://doi.org/10.4302/plp.v12i4.1054>.
- Lanh CV, Van TH, Van CL, Borzycki K, Khoa DX, Vu TQ, Trippenbach M, Buczyński R, Pniewski J. Supercontinuum generation in photonic crystal fibers infiltrated with nitrobenzene. *Laser Physics*. 2020;30(3):035105–9; Available from: <https://doi.org/10.1088/1555-6611/ab6f09>.
- Chu VL, Van TH, Van CL, Borzycki K, Khoa DX, Vu TQ, Trippenbach M, Buczyński R, Pniewski J. Optimization of optical properties of photonic crystal fibers infiltrated with chloroform for supercontinuum generation. *Laser Physics*. 2019;29(7):075107; Available from: [15.https://doi.org/10.1088/1555-6611/ab2115](https://doi.org/10.1088/1555-6611/ab2115).
- Lanh CV, Anuszkiewicz A, Ramaniuk A, Kasztelan R, Khoa XD, Trippenbach M, Buczyński RR. Supercontinuum generation in photonic crystal fibres with core filled with toluene. *Journal of Optics*. 2017;19(1):125604; Available from: <https://doi.org/10.1088/2040-8986/aa96bc>.
- Jones DJ, Diddams SA, Ranka JK, Stentz A, Windeler RS, Hall JL, Cundiff ST. Carrier-envelope phase control of femtosecond mode-locked lasers and direct optical frequency synthesis. *Science*. 2000;288(5466):635–639; PMID: 10784441. Available from: <https://doi.org/10.1126/science.288.5466.635>.
- Seddon AB. A prospective for new mid-infrared medical endoscopy using chalcogenide glasses. *International Journal of Applied Glass Science*. 2011;2(3):177–191; Available from: <https://doi.org/10.1111/j.2041-1294.2011.00059.x>.
- Dudley JM, Genty G, Coen S. Supercontinuum generation in photonic crystal fiber. *Reviews of Modern Physics*. 2006;78:1135–1184; Available from: <https://doi.org/10.1103/RevModPhys.78.1135>.
- Paulsen HN, Hilligse KM, Thogersen J, Keiding SR, Larsen JJ. Coherent anti-Stokes Raman scattering microscopy with a photonic crystal fiber based light source. *Optics Letters*. 2003;28(13):1123–1125; PMID: 12879928. Available from: <https://doi.org/10.1364/OL.28.001123>.
- Sanders S. Wavelength-agile fiber laser using group-velocity dispersion of pulsed super-continua and application to broadband absorption spectroscopy. *Applied Physics B*. 2002;75:799–802; Available from: <https://doi.org/10.1007/s00340-002-1044-z>.
- Povazay B, Bizheva K, Unterhuber A, Hermann B, Sattmann H, Fercher AF, Drexler W, Apolonski A, Wadsworth WJ, Knight JC, Russell PS, Vetterlein M, Scherzer E. Submicrometer axial resolution optical coherence tomography. *Optics Letters*. 2002;27(20):1800–1802; PMID: 18033368. Available from: <https://doi.org/10.1364/OL.27.001800>.
- Morioka T, Mori K, Kawanishi S, Saruwatari M. Multi-WDM-channel Gbit/s pulse generation from a single laser source utilizing LD-pumped supercontinuum in optical fibers. *IEEE Photonics Technology Letters*. 1994;6(3):365–368; PMID: 35502650. Available from: <https://doi.org/10.1109/68.275490>.
- Barh A, Ghosh S, Agrawal GP, Varshney RK, Aggarwal ID, Pal BP. Design of an efficient mid-IR light source using chalcogenide holey fibers: a numerical study. *Journal of Optics*. 2013;15(3):035205; Available from: <https://doi.org/10.1088/2040-8978/15/3/035205>.
- Dudley JM, Taylor JR. Supercontinuum generation in optical fibers. Cambridge University Press. 2010; Available from: <https://doi.org/10.1017/CBO9780511750465>.
- Shiryaev V, Churbanov M. Trends and prospects for development of chalcogenide fibers for mid-infrared transmission. *Journal of Non-Crystalline Solids*. 2013;377:225–230; Available from: <https://doi.org/10.1016/j.jnoncrysol.2012.12.048>.
- Slusher RE, Lenz G, Hodelin J, Sanghera J, Shaw LB, Aggarwal ID. Large Raman gain and nonlinear phase shift in high-purity As₂Se₃ chalcogenide fibers. *Journal of the Optical Society of America B*. 2004;21(6):1146–1155; Available from: <https://doi.org/10.1364/JOSAB.21.001146>.
- Asobe M, Kanamori T, Kubodera K. Applications of highly nonlinear chalcogenide glass. *IEEE Journal of Quantum Electronics*. 1993;29(8):2325–2333; Available from: <https://doi.org/10.1109/3.245562>.
- Saini TS, Kumar A, Sinha RK. Broadband mid-IR supercontinuum generation in As₂Se₃ based chalcogenide photonic crystal fiber: a new design and analysis. *Optics Communications*. 2015;347:13–19; Available from: <https://doi.org/10.1016/j.optcom.2015.02.049>.
- Zhao T, Lian Z, Benson T, Wang X, Zhang W, Lou S. Highly-nonlinear polarization-maintaining As₂Se₃-based photonic quasi-crystal fiber for supercontinuum generation. *Optical Materials*. 2017;73:343–349; Available from: <https://doi.org/10.1016/j.optmat.2017.07.010>.
- Karim MR, Ahmada H, Ghosh S, Rahman BMA. Mid-infrared supercontinuum generation using As₂Se₃ photonic crystal fiber and the impact of higher-order dispersion parameters on its supercontinuum bandwidth. *Optical Fiber Technology*. 2018;45: 255–266; Available from: <https://doi.org/10.1016/j.yofte.2018.07.024>.
- Wang Y, Dai S, Han X, Zhang P, Liu Y, Wang X, Sun S. Broadband mid-infrared supercontinuum generation in novel As₂Se₃-As₂Se₂ step-index fibers. *Optics Communications*. 2018;410:410–415; Available from: <https://doi.org/10.1016/j.optcom.2017.10.056>.
- Gao W, Zhang X, Jiang W, Zhang Z, Gao P, Chen L, Wang P, Zhang W, Wang R, Liao M, Suzuki T, Ohishi Y, Zhou Y. Characteristics of vector beams in mid-infrared waveband in an As₂Se₃ photonic crystal fiber with small hollow core. *Opti-*

- cal Fiber Technology. 2020;55:102152;Available from: <https://doi.org/10.1016/j.yofte.2020.102152>.
29. Lanh CV, Thuy NT, Bao Tran LT, Duc HT, Ngoc VTM, Hieu VL, Van TH. Multi-octave supercontinuum generation in As₂Se₃ chalcogenide photonic crystal fiber. *Photonics and Nanostructures - Fundamentals and Applications*. 2022;48:100986;Available from: <https://doi.org/10.1016/j.photonics.2021.100986>.
 30. Cherif R, Salem AB, Zghal M, Besnard P, Chartier T, Brilland L, Troles J. Highly nonlinear As₂Se₃-based chalcogenide photonic crystal fiber for midinfrared supercontinuum generation. *Optical Engineering*. 2010;49(9):095002–6;Available from: [10.1117/1.3488042](https://doi.org/10.1117/1.3488042).
 31. Chen A, Yu Z, Dai B, Li Y. Highly sensitive detection of refractive index and temperature based on liquid-filled D-shape PCF. *IEEE Photonics Technology Letters*. 2021;33(11):529–532;Available from: <https://doi.org/10.1109/LPT.2021.3073425>.
 32. Agrawal G. Chapter 2-pulse propagation in fibers, *Nonlinear Fiber Optics* (4th edition). Academic Press 2006:25–50;PMID: 16455588. Available from: <https://doi.org/10.1016/B978-012369516-1/50002-9>.
 33. Dabas B, Sinha R. Dispersion characteristic of hexagonal and square lattice chalcogenide As₂Se₃ glass photonic crystal fiber. *Optics Communications*. 2010;283(7):1331–1337;Available from: <https://doi.org/10.1016/j.optcom.2009.11.091>.
 34. Wei C, Zhang H, Hongxi HL, Liu SY. Broadband mid-infrared supercontinuum generation using a novel selectively air-hole filled As₂S₅-As₂S₃ hybrid PCF. *Optik*. 2017;141:32–38;Available from: <https://doi.org/10.1016/j.ijleo.2017.02.061>.